RARE EARTH ELEMENTS AND THEIR ISOTOPES IN THE OCEAN

Y. Nozaki, University of Tokyo, Tokyo, Japan

Introduction

The rare earth elements comprise fifteen lanthanide elements (atomic number, $Z = 57$–71) as well as yttrium ($Z = 39$) and scandium ($Z = 21$), although promethium ($Z = 61$) does not appear in nature due to its radioactive instability (**Figure 1**). They are an extremely coherent group in terms of chemical behavior and have recently been subjected to intense investigation in the field of marine geochemistry. All rare earth elements occur as a trivalent state with exception of Ce^{4+} and Eu^{2+}. In the lanthanide series, the progressive filling of electron in the shielded inner 4f shell with increasing atomic number leads to gradual decrease in the ionic radii from La^{3+} to Lu^{3+}, which is called 'the lanthanide contraction'. Consequently, small but systematic changes in chemical properties allow them to be used for unique tracers in studying fundamental processes that govern the cycling of rare earth elements in the ocean. For instance, the heavier lanthanides were predicted to be more strongly complexed in seawater and hence more resistant to removal by scavenging of particulate matter. Yttrium mimics the heavy lanthanides, particularly holmium, because of similarity in the ionic radii. However, Sc is a substantially smaller cation with a geochemical behavior that differs from other rare earths. In most literature, therefore, 'rare earth elements (REEs)' generally include only lanthanides and Y, and Sc is treated separately.

Two elements, Ce and Eu can take the other oxidation states. Although Ce is generally well accommodated within the strictly trivalent lanthanide series in igneous rocks, oxidation reaction of Ce^{3+} to Ce^{4+} proceeds in oxygenated aqueous systems. In seawater, the resulting Ce^{4+} hydrolyzes readily and tends to be removed by scavenging. For this reason, seawater is typically depleted in Ce relative to that expected from neighboring La and Pr, whereas Ce is often enriched in some authigenic minerals such as manganese nodules and phosphorites. Europium can be reduced to Eu^{2+}, a larger cation that can be segregated from other REEs, during magmatic processes. Anomalous concentrations of Eu are not uncommon in various igneous and sedimentary rocks. However reduction of Eu does not normally take place within the ocean, although an Eu enrichment has often be encountered in hydrothermal fluids venting at midoceanic ridges. The anomalous behavior of Ce due to oxidation–reduction reactions can be best and quantitatively evaluated relative to the trivalent neighbors (La and Pr) in the lanthanides series without significant influence of the other processes affecting their oceanic distributions. This is a notable advantage of the element over the other transition metals, such as Mn and Fe, which behave individually affected by the oxidation states.

In addition, there are two geochemically important isotopes of the lanthanides, ^{143}Nd and ^{138}Ce. The ^{143}Nd is produced by decay of ^{147}Sm with a half-life of 10.6×10^{11} years. Natural variation of $^{143}Nd/^{144}Nd$ in terrestrial materials occurs depending on mantle/crust segregation of Sm and Nd, and the age of the rocks. Thus, the $^{143}Nd/^{144}Nd$ ratio may be used to constrain the sources of the REEs and mixing within the ocean. Likewise, the $^{138}Ce/^{142}Ce$ ratio may also be used to constrain homogenization of the element by oceanic mixing since the ^{138}Ce is produced by ^{138}La decay (half-life, 2.97×10^{11} years). However, the $^{138}Ce/^{142}Ce$ ratio has not been well exploited in marine geochemistry yet, because of its smaller natural variation as compared to that of Nd isotopes and analytical difficulty.

History and REE Normalization

The analysis of picomolar REE concentrations in seawater has been difficult due to lack of sensitivity in the conventional methods. Earlier attempts to measure REEs relied almost entirely on high-sensitivity instrumental neutron activation analysis. In 1963 reliable REE concentrations were reported in a few waters from the Eastern Pacific as well as those in a manganese nodule and a phosphorite and their significance was recognized. Basic features of the REEs in seawater were found: a progressive increase across the lanthanide series from the light Pr to the heaviest Lu when the seawater concentrations were divided by those of sediments, and that Ce is markedly depleted in the seawater but enriched in the manganese nodule relative to neighboring La and Pr, as expected from its $4+$ valency
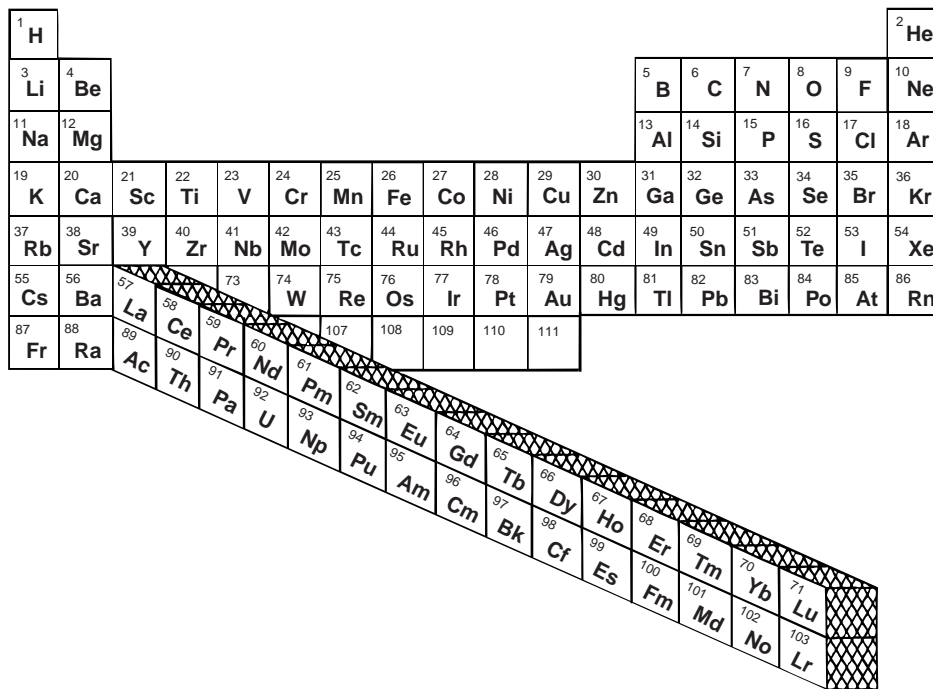
Figure 1 Periodic table showing the position of rare earth elements.

state. Europium was normal relative to other trivalent REEs in all the sample. It was also noted that the concentrations of the heavy REEs (Ho, Yb and Lu) in the Pacific deep water were considerably higher than those in the surface water. Although these earlier findings had to be refined and confirmed by subsequent workers with more precise modern techniques, the fundamental aspects of the REE marine geochemistry were developed for that time. Prior to 1980, reliable data on the distribution of REEs in seawater were few. Since the early 1980s, a growing number of reports on the subject have become available. Now, several laboratories in the world are capable of determining REEs in seawater with precision between one and a few percent by use of isotope dilution thermal ionization mass spectrometry (ID-TIMS) or inductively coupled plasma mass spectrometry (ICPMS). Therefore, more detailed arguments are possible regarding geochemical processes controlling the concentration, distribution, fractionation and anomalous behaviors in the oceans.

When REE fractionation is discussed, it is common to normalize the data to the values in shale which are thought to be representative of the REEs in the upper continental crust. The shale-normalization not only helps to eliminate the well-known distinctive even–odd variation in natural abundance (the Oddo–Harkins effect) of REEs but also visual-izes, to a first approximation, fractionation relative to the continental source. It should be noted, however, that different shale values in the literature have been employed for normalization, together with the ones of the Post-Archean Australian Sedimentary rocks (PAAS) adopted here (**Table 1**). Thus, caution must be paid on the choice of the shale values if one ought to interpret small anomalies at the strictly trivalent lanthanides such as Gd and Tb. Alternatively, for detailed arguments concerning fractionation between different water masses in the ocean, it has been recommended that the data are normalized relative to the REE values of a distinctive reference water mass, for example, the North Pacific Deep Water (NPDW, **Table 1**). The NPDW-normalization eliminates the common features of seawater that appeared in the shale-normalized REE pattern and can single out fractionation relative to the REEs in the dissolved end product in the route of the global ocean circulation.

The Oceanic Distributions

In 1982, the first 'oceanographically consistent' vertical profiles were reported for nine out of ten lanthanides that could be measured by the ID-TIMS method in the North Atlantic. Since then, a signifi-cant amount of data on the distribution of REEs have accumulated from various oceanic regions. For

Table 1 Ionic radii and the average REE concentrations in shale and seawater used for normalization

Element	Atomic number Z	Ionic Radius (Å)[a]		PAAS[a] (μmol/kg)	NPDW[b] (pmol/kg)
		CN = 6	CN = 8		
Y	39	0.900	1.019	304	236.3
La	57	1.032	1.160	275	38.7
Ce	58	1.010	1.143	568	3.98
Pr	59	0.990	1.126	62.7	5.10
Nd	60	0.983	1.109	235	23.8
Sm	62	0.958	1.079	36.9	4.51
Eu	63	0.947	1.066	7.1	1.24
Gd	64	0.938	1.053	29.6	6.83
Tb	65	0.923	1.040	4.9	1.13
Dy	66	0.912	1.027	28.8	8.38
Ho	67	0.901	1.015	6.0	2.34
Er	68	0.890	1.004	17.0	7.94
Tm	69	0.880	0.994	2.4	1.23
Tb	70	0.868	0.985	16.3	8.37
Lu	71	0.861	0.977	2.5	1.46

[a]After Taylor and McLennan (1985) for trivalent cations; CN, coordination number.
[b]Dissolved ($< 0.04\,\mu m$) REE in the North Pacific Deep Water at $2500 \pm 100\,m$ (after Alibo and Nozaki, 1999).

example, **Figure 2** shows the station locations where the REEs were measured in seawater, together with the Nd concentrations in the surface water. Some of them are based on filtered samples, using generally a $0.4–1.0\,\mu m$ membrane, of which results are called 'dissolved' concentrations. Many others, however, were measured on unfiltered and acidified seawaters, and hence can be ascribed to 'acid-soluble total'
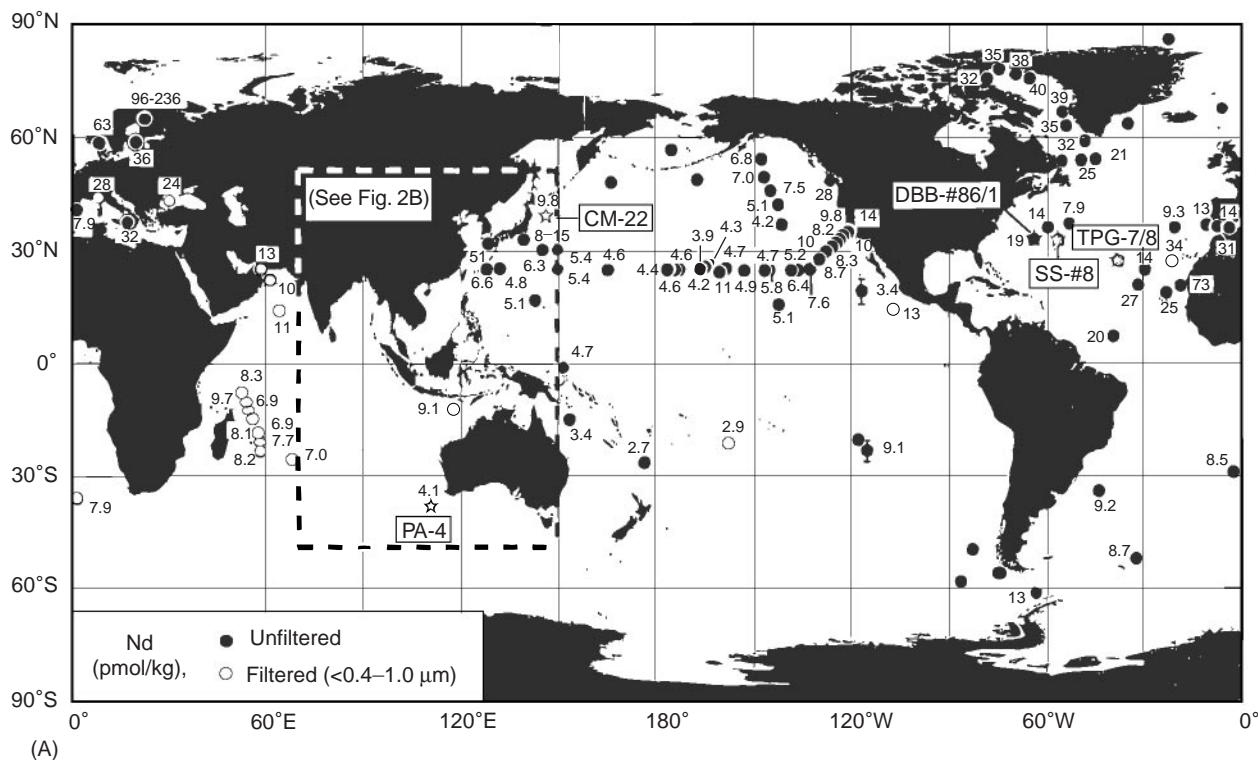

Figure 2 (A) World map for the REE data in the literature (Byrne and Sholkovitz, 1996) and Nd concentrations in the surface water ($< 100\,m$ in depth). The open and filled circles indicate the locations where filtered and unfiltered samples were analyzed. The stars indicate the station locations for which the profile data are shown in **Figure 3**.
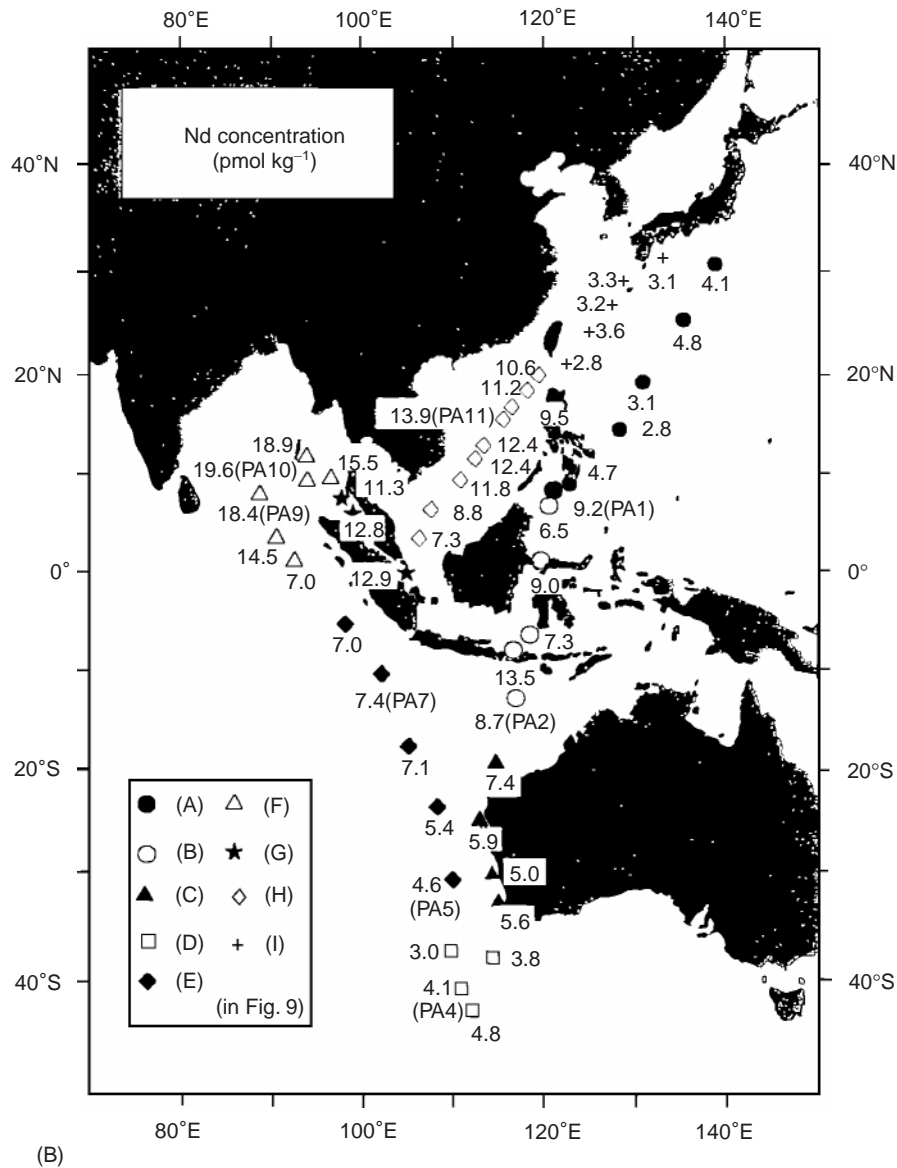
Figure 2 *Continued* (B) The station locations occupied by R. V. Hakuho Maru during the 1996/97 Piscis Austrinus Expedition and the dissolved ($< 0.04\,\mu m$) Nd concentrations in the surface waters. The different symbols are used according to the different regions where NPDW-normalized REE patterns are grouped in **Figure 9**. The stations indicated by PA-numbers show the locations where the vertical profiles of dissolved REEs were determined.

concentrations. The difference between the two is generally small, less than 5% for all trivalent REEs in the open oceans, even if the finer $0.04\,\mu m$ membrane is used for filtration (**Table 2**), and gross features of their vertical profiles remain unchanged. Nevertheless, when fine structures of the REE patterns are discussed, filtration becomes critical in changing the pattern since the particulate fraction decreases from $\sim 5\%$ at the light and middle to less than 1% at the heavy REEs. Furthermore, there is an obvious exception for Ce of which more than 35% is associated with particles, being consistent with its $4+$ oxidation state. Also, the REEs in unfiltered samples close to the bottom often show anomalously high concentrations due to resuspension of underlying sediments.

The vertical profiles of dissolved ($< 0.04\,\mu m$) REEs for different oceanic basins are shown in **Figure 3**. Except for Ce, all REEs show 'nutrient-like' gradual increase with depth. There are small but systematic differences in the profiles across the series, although the North Atlantic profiles show somewhat complex features dominated by horizontal advection of different water masses (from the

Table 2 Rare earth elements associated with particulate matter in seawater

Atomic number Z	Element	Particulate fraction (%)			
		N.W. Pacific[a]	W. Indian Ocean[b]	N. Atlantic[c]	Average
39	Y	0.8 ± 1.6	–	–	0.80
57	La	2.9 ± 2.2	1.33 ± 0.67	3.68 ± 0.27	2.65
58	Ce	36.6 ± 7.6	17.1 ± 4.1	23.7 ± 7.6	25.8
59	Pr	5.5 ± 3.4	–	–	5.49
60	Nd	4.4 ± 2.7	2.10 ± 0.65	3.42 ± 0.66	3.31
62	Sm	5.1 ± 2.9	2.10 ± 0.63	2.75 ± 0.69	3.30
63	Eu	5.4 ± 5.6	1.50 ± 0.37	3.00 ± 0.58	3.30
64	Gd	4.8 ± 3.1	1.28 ± 0.33	1.70 ± 0.27	2.58
65	Tb	4.2 ± 3.7	(1.2)[d]	(1.6)[d]	2.33
66	Dy	2.8 ± 3.2	1.03 ± 0.35	1.55 ± 0.33	1.80
67	Ho	0.81 ± 3.0	(0.80)[d]	(1.1)[d]	0.90
68	Er	0.45 ± 3.3	0.57 ± 0.19	0.63 ± 0.45	0.55
69	Tm	–	(0.50)[d]	(0.62)[d]	0.56
70	Yb	–	0.48 ± 0.20	0.61 ± 0.33	0.55
71	Lu	–	0.44 ± 0.21	0.48 ± 0.34	0.46

[a]Acid-soluble particulate fraction (> 0.04 μm), after Alibo and Nozaki (1999).
[b]Based on analysis on particulate matter collected on 0.4 μm membrane filters (Bertram and Elderfield, 1994).
[c]Sum of analyses on successive chemical treatments on 0.4 μm-filtered particles (Sholkovitz *et al.* 1994).
[d]Estimated value from neighboring trivalent REEs.

above, the Sargasso Sea Surface Water, the North Atlantic Deep Water, and the Antarctic Bottom Water). For instance, in the Southern Ocean and the North Pacific, the light and middle REEs (e.g. Pr-Gd) almost linearly increase with depth, whereas the heavy REEs (e.g. Ho-Lu) and Y show convex features. The concentrations of the heavy REEs below 1500 m are in the order of North Atlantic < Southern Ocean < North Pacific much like those of nutrients, whereas those of the light REEs are Southern Ocean < North Atlantic < North Pacific, presumably reflected by scavenging intensities in those regions. Although the vertical profiles of the REEs are similar to those of nutrients, e.g. dissolved silica, there is a difference in that the REE concentrations never approach zero in the surface water like nutrients in the temperate oligotrophic zone. Analysis of interelement correlations indicate that the heavy REEs and Y better correlate with dissolved silica and alkalinity than with nitrate and phosphate. Within the REEs, the best correlations ($R^2 > 0.99$) can be found between neighboring trivalent REEs, and between Y and the heavy REEs. As a trivalent REE pair is apart in their atomic number, the correlation between the two becomes worse. Lanthanum often deviates in these general trends from the light REEs toward the heavy REEs.

The vertical profiles of Ce is unique among the REEs showing a decrease from the high concentrations in the surface waters to the low and nearly constant values in the deep waters (**Figure 3**). Such a distribution pattern can be seen for other least-soluble elements, such as Al, Co, and Bi which also hydrolyze readily. The different profiles among the basins may be governed by the balance in the strength of external inputs (eolian + riverine) to the surface ocean and particle scavenging throughout the water column.

REE Patterns

Shale-normalized dissolved REE patterns for the western North Pacific are shown in **Figure 4(A)**. Generalized features common to all seawaters are: a progressive heavier REE enrichment relative to the lighter ones and a pronounced depression at Ce. These features can be best understood by the conceptual model for interactions between REEs in solution and particles and subsequent removal of particulate matter by settling (**Figure 5**). The former is ascribed to a systematic increase in stability constant with atomic number of complexes of REE-ligands (mainly carbonate) in seawater. The latter is explained by preferential removal of Ce^{4+} species from seawater relative to trivalent REEs. It is also noted that La is always enriched compared to that expected by extrapolation from heavier Pr and Nd. Furthermore, the increasing trend from the light to the heavy REE is nonlinear and often has a marked break between Gd and Tb. These less-pronounced features have been discussed in terms of the basic physicochemical characteristics relating to absence
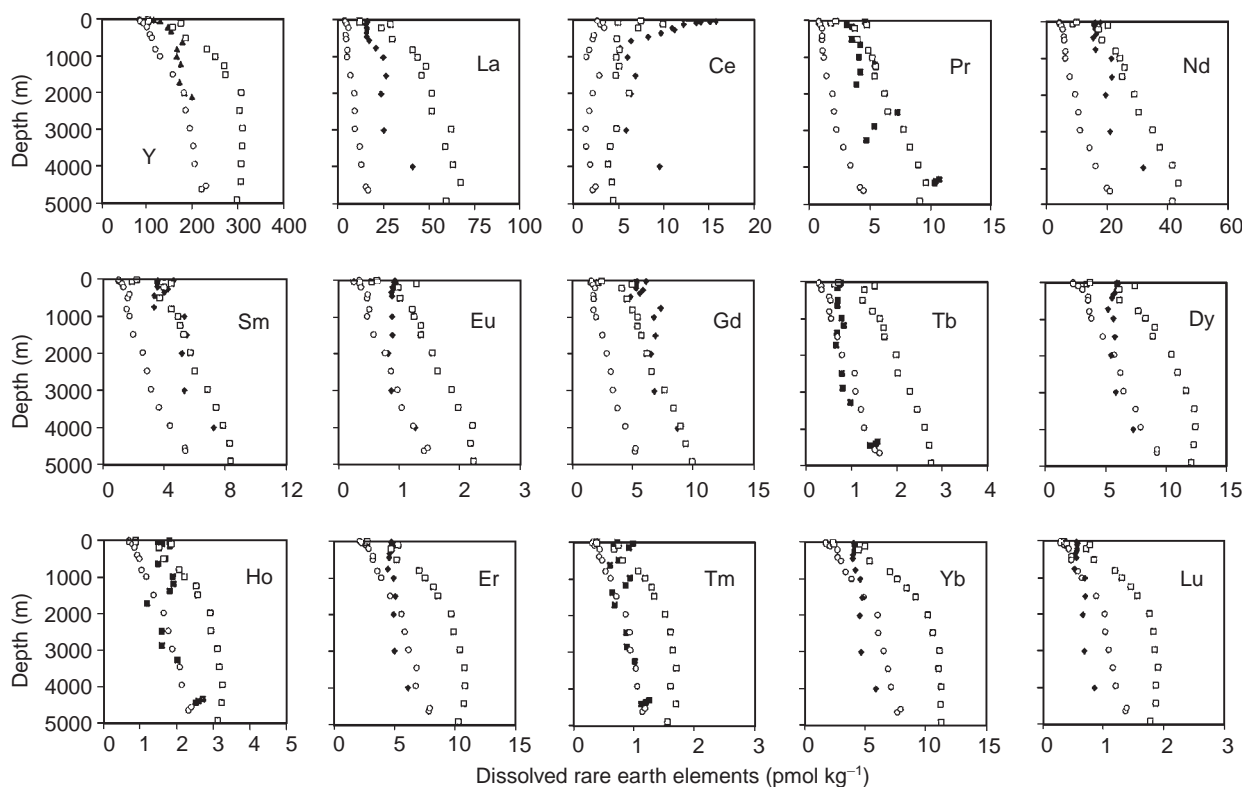
Figure 3 The vertical profiles of dissolved ($< 0.04\,\mu m$) REEs in the western North Pacific (CM-22; □), and the Southern Ocean (PA-4; ○) from Alibo and Nozaki, unpublished. The North Atlantic profile data based on dissolved ($< 0.4\,\mu m$) REEs (SS-#8; ◆) from Sholkovitz and Schneider (1991) and acid-soluble total concentrations for monoisotopic REEs (DBB-#86/1; ■) from De Baar *et al.* (1983) and yttrium (TPG-7/8; ▲) from Alibo *et al.* (1999).

for La and half filled for Gd of 4f electrons. However, the reasoning is somewhat controversial and has not yet been confirmed.

The NPDW-normalized REE patterns in the water column of the western North Pacific are shown in **Figure 4(B)**. In comparison with **Figure 4(A)**, it generally shows a flat pattern (no fractionation) including those between 400 and 600 m where the North Pacific Intermediate Water (NPIW) penetrates. The exception is that the surface samples ($< 200\,m$) indicate a middle REE enriched pattern being reflected by the sources and fractionation during scavenging of REEs. The different water masses have unique NPDW-normalized patterns (**Figure 6**). Thus, the REE patterns are useful as tracers in defining those water masses.

Redox Reaction of Ce, and Ce Anomalies

Cerium is oxidized in seawater according to the following equation,

$$Ce^{3+} + 2H_2O = CeO_2 + 4H^+ + e^-$$
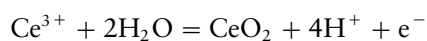
where CeO_2 is highly insoluble species and rapidly removed by scavenging. This oxidation is considered to occur mainly in the surface water through bacterial mediation. There is no evidence that Ce oxidation continues in the deep sea. The deviation of Ce from other trivalent REEs in geochemical behavior is generally expressed as 'Ce-anomaly' which is defined by the following equation,

$$Ce/Ce^* = 2[Ce]/([La] + [Pr])$$

or

$$Ce/Ce^* = 3[Ce]/([La] + 2[Nd])$$

where [] indicates shale-normalized value of the REE concentration. The negative Ce-anomaly implies $Ce/Ce^* < 1$, vice versa. In the open oceans, the negative Ce-anomaly is developed with increasing depth (**Figure 7**) because of a decrease in Ce coinciding with increases in La and Pr (or Nd) concentrations.

In the aoxic basins, Ce^{4+} is reduced to Ce^{3+} and the Ce-anomaly tends to be smaller than those in
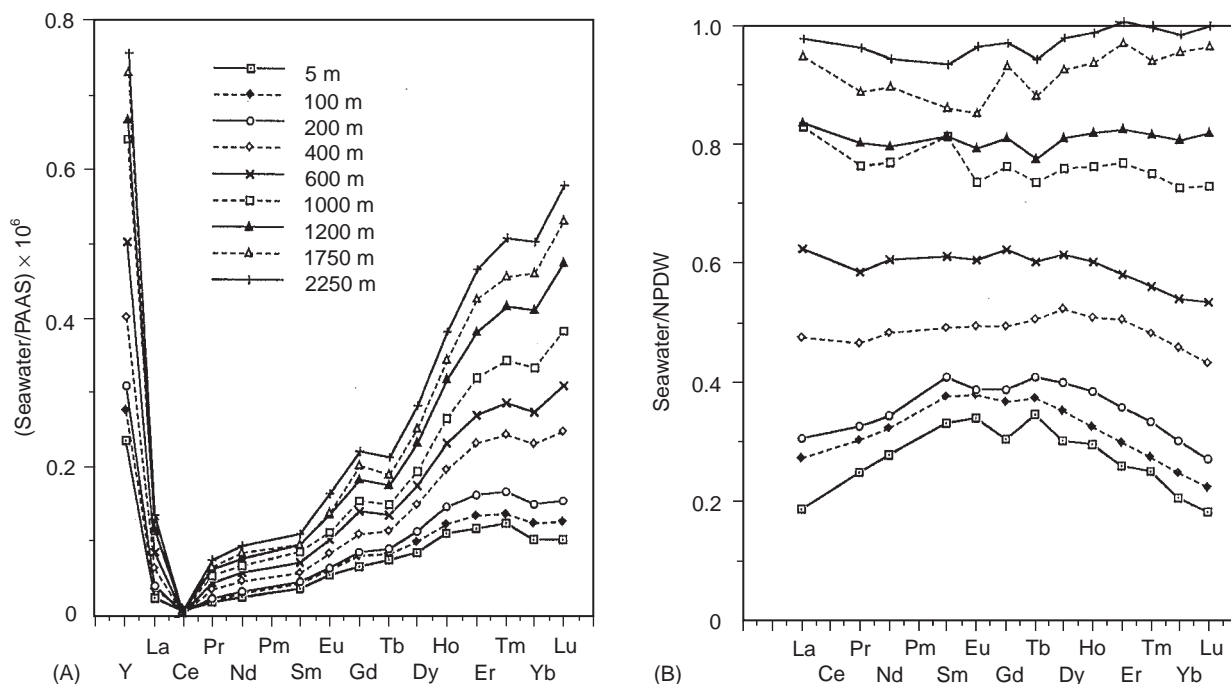
Figure 4 The PAAS-normalized (A) and the NPDW-normalized (B) patterns of dissolved REEs in the western North Pacific (Alibo and Nozaki, 1999).

oxygenated waters. The Black Sea provides a best example in which Ce/Ce* sharply increases from less than 0.1 at the oxic/aoxic boundary of $\sim 100\,m$ depth to ~ 1.0 (no anomaly) in reducing waters

below 200 m (**Figure 8**). Even positive Ce anomaly can be found in the deep Cariaco Trench. Cerium reduction also takes place in coastal and
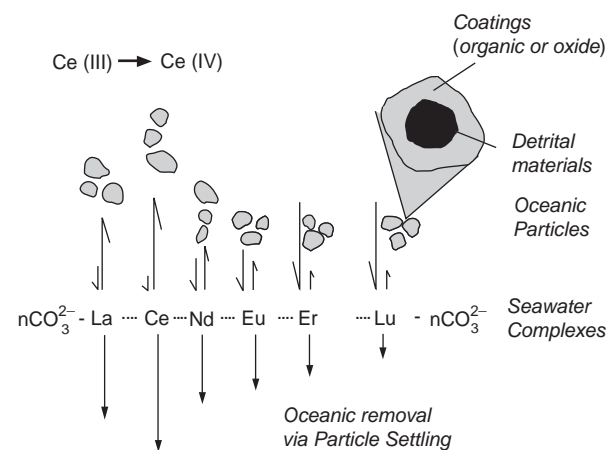

Figure 5 A conceptual model of REE fractionation between particles and seawater. Main features include (1) the systematic variation in the relative affinity of trivalent REEs for complexation to solution carbonates and binding to particles, (2) the enhanced formation of particulate Ce due to the oxidation of Ce(III) to Ce(IV), and presence of surface active coatings on detrital particles. These features lead to fractionation of REE between seawater and particles and to fractionation via the settling of large particles. After Sholkovitz et al. (1994).
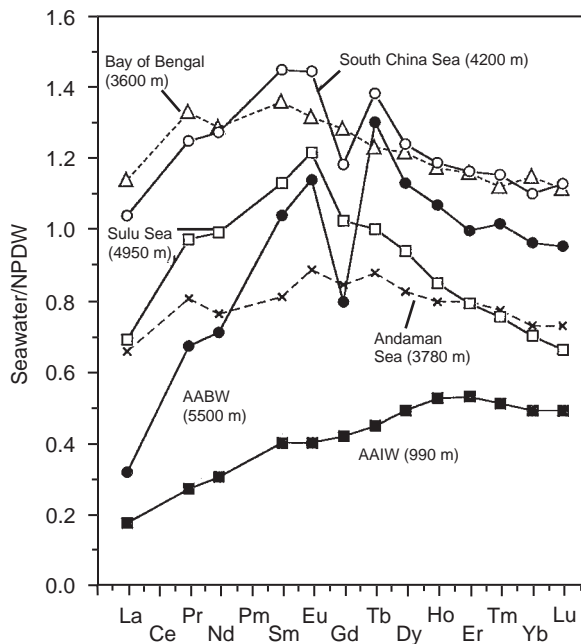

Figure 6 The characteristic features of NPDW-normalized patterns of dissolved REEs in different oceanic basins. Data from Alibo and Nozaki (unpublished) and Nozaki et al. (1999).
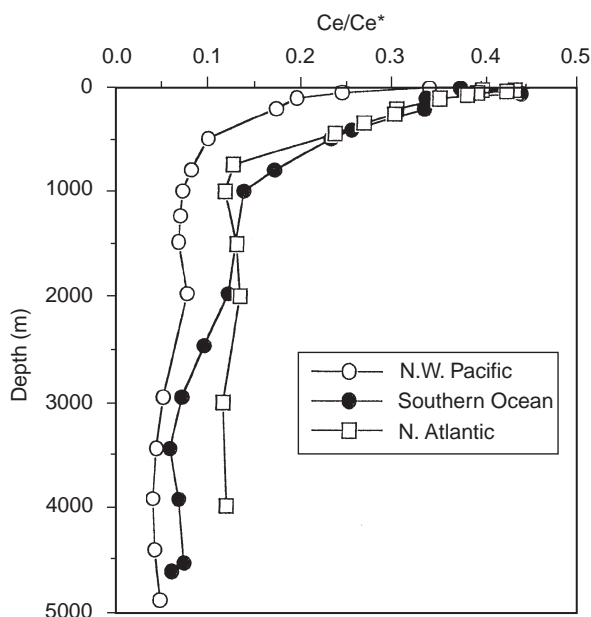
Figure 7 The vertical profiles of Ce-anomaly calculated from the profile data in **Figure 3**.

hemipelagic sediment pore waters and can affect the distribution of Ce in the overlying waters.

Inputs of REEs to the Ocean

The most obvious source of REEs in the ocean is riverine input. The concentrations of dissolved REEs in river waters are significantly higher than those of seawaters. The behaviors of the dissolved REEs in rivers and estuaries have been intensively studied as a link of REE geochemistry between the crust and the ocean. Shale-normalized REE patterns in river and estuarine waters often show nonflat patterns indicating that fractionation takes place with respect to continental crust. One of the prominent features derived from those works is that large-scale removal of dissolved REEs (in particular, light REEs) occurs in the estuarine mixing zone. Planktonic uptake, coprecipitation with iron hydroxides, and salt-induced coagulation of colloids have been suggested as the removal mechanism. This reduces the effective fluvial flux of dissolved REEs to the ocean considerably and affects the budget calculation in the ocean. For example, the river flux of dissolved Nd is estimated to be 4.6×10^6 mol year^{-1} (**Table 3**), being lowered by a factor of 3–4 in the estuaries, and the mean oceanic residence time with respect to the river input is about 10^4 years. This Nd mean residence time appears too long in the light of heterogeneous distribution of its isotopic composition observed in the different oceanic basins.

The ^{143}Nd/^{144}Nd isotopic composition is generally expressed as,

$$\varepsilon_{\text{Nd}} = \left[\frac{(^{143}\text{Nd}/^{144}\text{Nd})_{\text{measured}}}{0.512638} - 1 \right] \times 10^4$$

where the value of 0.512638 is referred to the ^{143}Nd/^{144}Nd ratio in the chondritic uniform reservoir (CHUR). Rivers entering into the Atlantic Ocean are influenced by old continental crust and have a relatively nonradiogenic ε_{Nd} value of -12, whereas values for rivers entering into the Pacific which is surrounded by young oceanic islands and island arcs are more radiogenic, -3 to -4. Rivers draining into the Indian Ocean have intermediate values around -9. The Nd isotopic compositions in the riverine input are almost faithfully reflected in seawater. The measured ε_{Nd} values for seawater also average -12 ± 2.5 for the Atlantic, -8 ± 2 for the Indian Ocean, and -3 ± 2 for the Pacific Ocean. Thus, the mean residence time of Nd must be short compared with the oceanic mixing time of $\sim 10^3$ years. This is in contrast to the Sr isotopes which show a constant ^{87}Sr/^{86}Sr ratio in seawater because of homogenization by oceanic mixing during its residence time of $\sim 10^6$ years. Some additional sources of REEs appear to exist in the ocean to maintain geochemical consistency for Nd isotopes.

The concentrations of REEs in hydrothermal fluids venting from hot springs at mid oceanic ridges have recently been investigated. They are generally 1–2 orders of magnitude higher than those of ambient seawater with a distinctly positive Eu anomaly, but are also intensively removed by scavenging in the vicinity of hydrothermal vent fields. Consequently, the effective hydrothermal flux of REEs to the ocean is negligibly small compared to the fluvial flux.

Atmospheric input due to fallout of terrestrial aerosols and subsequent solubilization into seawater has been thought to be important, or even predominant in the open ocean for some reactive heavy metals such as iron and aluminum. However, the eolian fluxes are poorly quantified for the REEs as yet. Available estimates (**Table 3**), though highly uncertain, suggest that the eolian fluxes are 30–130% of the fluvial input of REEs. Terrestrial aerosols are transported through the atmosphere for relatively long distances from the sources by longitudinally prevailing winds such as the westerlies and the trade wind. This is in contrast to the fluvial input which enters the ocean across the land–sea interface. Thus, the relative importance of these REE sources may be reflected in the geographical
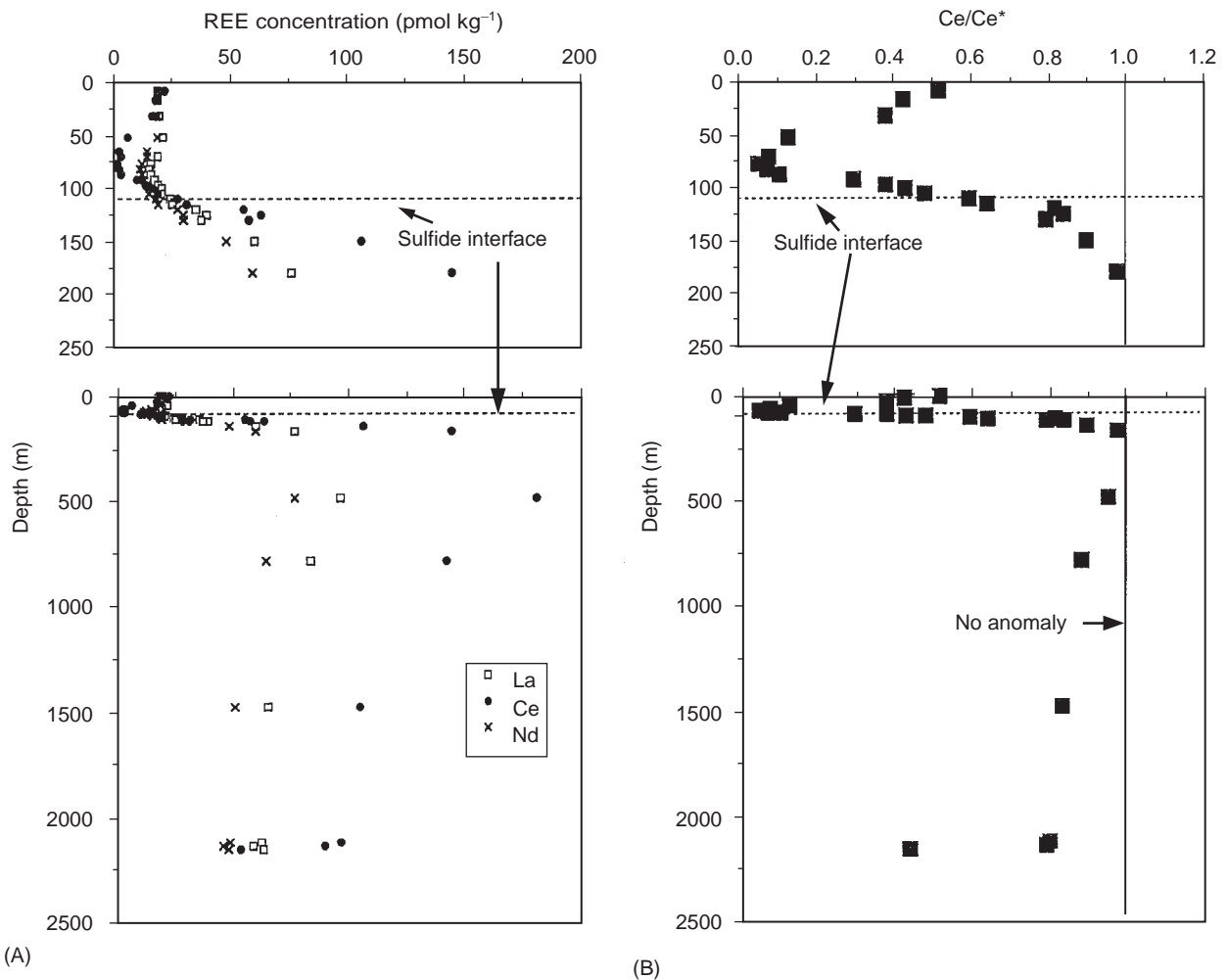
Figure 8 The vertical profiles of La, Ce, and Nd (A) and calculated Ce-anomaly (B) in the Black Sea. After German *et al.* (1991).

distribution of REEs in the surface waters. The distribution of dissolved Nd in the surface waters (**Figure 2**) shows the higher concentrations in regions of strong coastal influence, such as Baffin Bay, the Bay of Bengal, and the South China Sea. In the open ocean, there is a general tendency of Atlantic > Indian Ocean > Pacific for the surface dissolved Nd. The surface waters of the different oceanic province have different NPDW-normalized REE patterns due to the input of REEs from local terrigneous sources (**Figure 9**). The Nd isotopic composition (**Figure 10**) that can serve as a 'fingerprint' of REE source also varies significantly with location. The geographical distributions of Nd concentration and its isotopic composition, and the NPDW-normalized REE pattern are hardly explained by the pattern of prevailing winds. All suggest that the REEs are supplied to the ocean from local sources and their mean residence times in the surface waters are relatively short as compared to homogenization by lateral mixing.

The surface Nd distribution somewhat resembles that of fluvially and coastally derived [228]Ra with a half-life of 5.7 years which is predominantly supplied to the coastal and shelf waters from underlying sediments.

Since the direct riverine flux of dissolved Nd is not sufficient to yield its short mean residence time required for the oceanic Nd isotopic heterogeneity, some additional mechanism must be sought for the coastal and shelf sources of the REEs. Remineralization of REEs from river-transported sediments may occur near the coast and on the shelf. For instance, if only 1–2% of detrital Nd is released to the coastal water, then the mean oceanic residence time of Nd is shortened to less than 1000 years. In reality, there is some evidence that the REEs are released from sediments to the overlying water in the outer high-salinity regions of the Amazon and Fly River estuaries. Fractionation can also take place in the sediment diagenesis, and hence, makes the REE patterns

Table 3 Mean oceanic residence times derived from the particle reactivities and estimated remineralization fluxes of the REEs

Element	Mean dissolved concentration (C_d) (pmol kg^{-1})	Atmospheric flux[a] (10^6 mol y^{-1})	Riverine flux[a] (10^6 mol y^{-1})	Remineralization flux[b] (10^6 mol y^{-1})	Mean residence time (τ_{REE})[c] (y)
Y	220	8.3[d]	15[d]	155	1670
La	30	4.1	5.0	72	500
Ce	4.5	8.5	6.3	107	50
Pr	3.8	1.1[e]	1.2[e]	19	240
Nd	20	4.4	4.6	59	400
Sm	4.0	0.91	1.1	11	400
Eu	1.0	0.20	0.3	2.8	410
Gd	4.7	0.85	1.4	10	520
Tb	1.1	0.13[e]	0.22[e]	2.3	570
Dy	6.5	0.72	1.2	9.9	740
Ho	2.0	0.15[e]	0.27[e]	1.1	1820
Er	6.5	0.45	0.8	2.4	2420
Tm	1.0	0.055[e]	0.14[e]	0.36	2430
Yb	6.5	0.32	1.1	2.2	2440
Lu	1.3	0.058	0.2	0.35	2890

[a]After Greaves and Elderfield (1994). The values may be uncertain by a factor of 2–3.
[b]Remineralization flux $= (1.35 \times 10^9 \times C_d)/\tau_{REE}$ − Atmospheric flux − Riverine flux.
[c]Based on $\tau_{REE} = \tau_p/\alpha F_p$ for $\tau_p = 10$ years, $\gamma = 0.8 \pm 0.2$ and F_p values given in **Table 2**. The values may be uncertain by a factor of 2–3.
[d]Assumed to be 55 times of Ho flux from the crustal ratio.
[e]Estimated from neighboring trivalent REEs on the basis of shale (PAAS) composition.

of the surface waters different from those of river waters, depending upon the oceanic province. The highly radiogenic ε_{Nd} values observed near the Indonesian Archipelago (**Figure 10**) also suggest that erosion of volcanic islands can be an important source of REEs to the ocean. Although quantification of these local sources of REEs is difficult at present, the coastal and shelf mechanism appears to be significant in the balance of dissolved REEs in the ocean (**Table 3**).

Particle Reactivity and Mean Oceanic Residence Times of REEs

The major process that removes dissolved REEs from the water column is considered to be adsorptive scavenging by sinking particulate matter (**Figure 5**) which controls the distributions of not only REEs but also a number of reactive elements in the ocean. Some elements can also be removed by lateral transport along with currents and subsequent intensified particle scavenging and/or uptake at the sediment–water interface of the oceanic margins. This, 'boundary scavenging' is known to occur for ^{210}Pb and [231]Pa, but this mechanism is probably insignificant for dissolved REEs. The vertical profiles of dissolved REEs (**Figure 3**) strongly suggest that they are involved in the oceanic biogeochemical cycle.

Marine particulate matter comprises biogenic organic matter, opaline silica, and carbonates as well as inorganic oxides and terrestrial detritus. The biogenic particles are produced in the surface water and transported by settling to the deep water and the seafloor where they are largely remineralized to the water. Despite a rough similarity in the vertical profile between the REEs and dissolved Si or alkalinity, however, active processes such as biological uptake and incorporation of REEs into calcareous and opaline skeletons do not seem to play any important role in this respect. For instance, the REE concentrations of shells are extremely low. Also, it is unlikely that the dissolved REEs are actively taken up into organic tissues.

Adsorptive scavenging of reactive metals has been clearly demonstrated, since some short-lived radionuclides such as [234]Th, [210]Po and ^{210}Pb are highly enriched in particulate matter collected by filtration and sediment traps. The scavenging processes of reactive metals may be governed by competitive reactions between binding affinity onto the particle surfaces and complex formation with ligands in seawater (**Figure 5**). Although marine particles are composed of various materials, their surfaces are thought to be coated with organic matter and oxides of manganese and iron. The fine suspended particles, that can be conventionally collected by filtration, predominate in the surface area
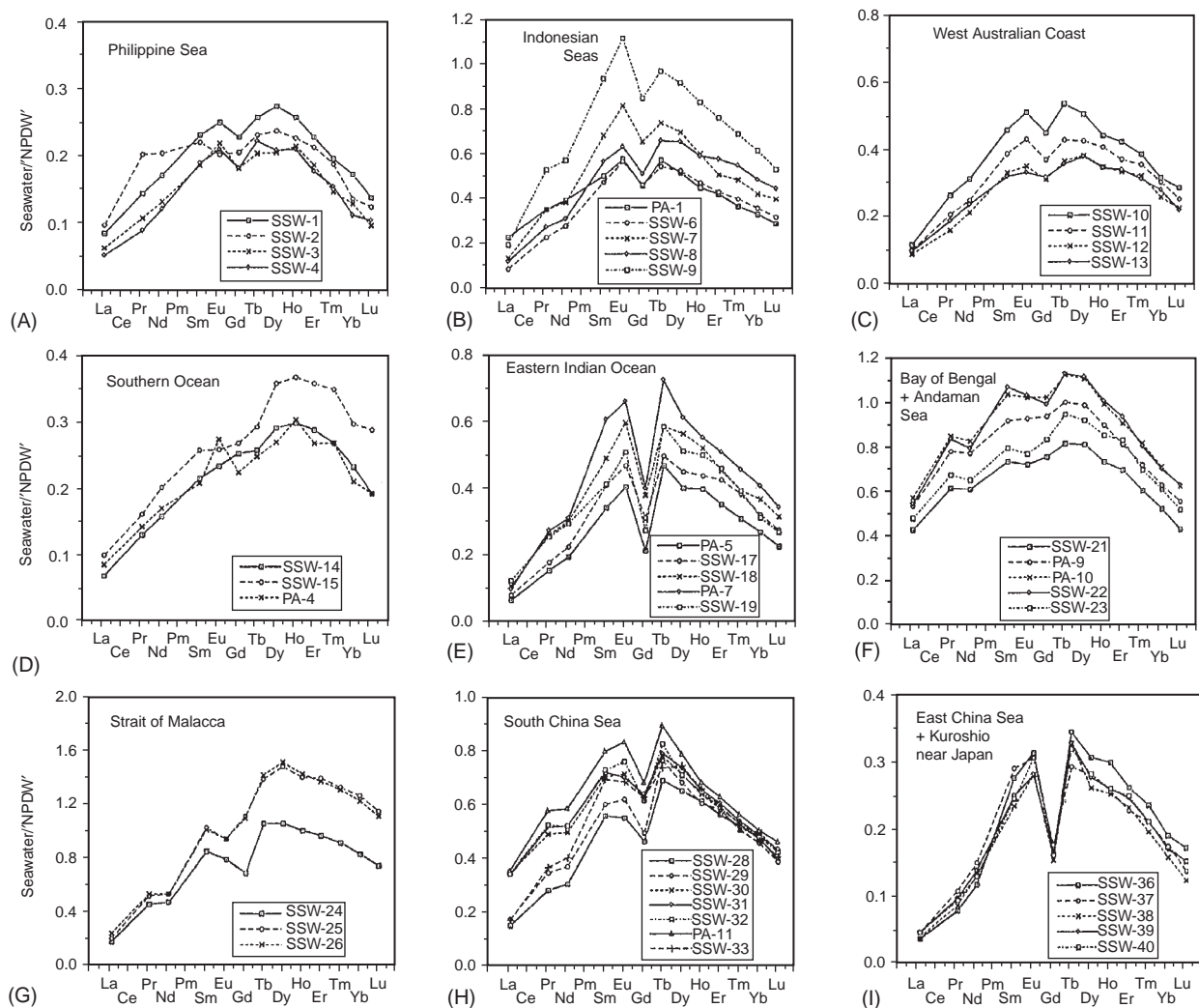
Figure 9 Comparison of NPDW-normalized REE patterns in the surface waters in the eastern Indian Ocean and its adjacent seas. See **Figure 2(B)** for the locations. Adapted from Amakawa *et al.* (2000).

onto which reactive metals are adsorbed and the standing stock of mass. In contrast, the large, fast sinking particles, that can be effectively collected by a sediment trap, virtually govern the vertical flux of materials. Those particles however, are frequently exchanged through aggregation and disaggregation during sinking through the water column. Since the vertical transport of particulate matter to the sedimentary sink is a process common to all associated elements, the overall rate of removal from the ocean for metals such as the REEs must depend on their partitioning between dissolved and particulate phases and a mean sinking velocity of the particles. Available data on the REEs associated with suspended particles are summarized in **Table 2**.

With the assumptions that a large portion of particulate REEs are exchangeable with dissolved REEs

and that the suspended fine particles are incorporated into the large, fast-sinking particles through repeated aggregation and disaggregation and eventually removed from the ocean with a certain mean residence time (τ_p), the mean residence time of REEs (τ_{REE}) is given by the following equation.

$$\tau_{REE} = \tau_p/\gamma F_p$$

where F_p is the fraction of particulate REEs in seawater (**Table 2**) and γ is the portion that is effectively exchangeable with the dissolved REEs. Based on the studies of Th isotopic systematics in the water column, the fine particles, on which most reactive metals reside, settle with a mean speed of $\sim 1 \, m \, day^{-1}$ corresponding to the mean oceanic residence time of about 10 years. From the chemical
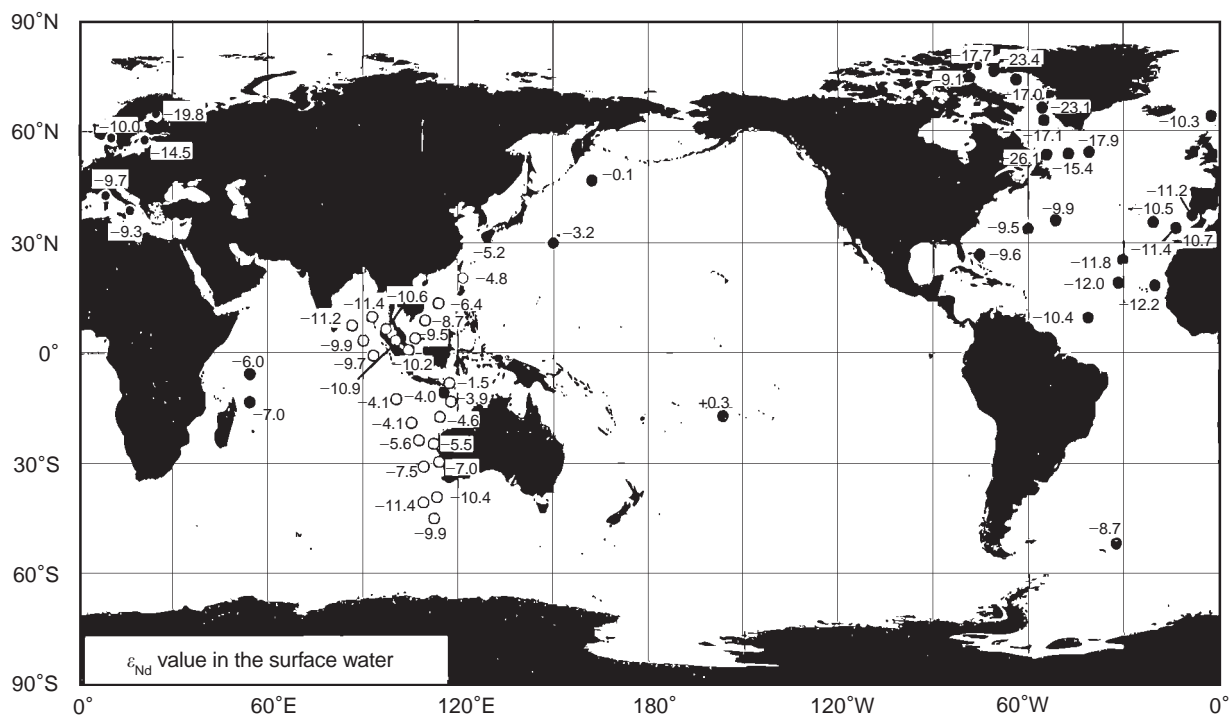
Figure 10 The distribution of $^{143}Nd/^{144}Nd$ isotopic composition (expressed as ε_{Nd} value) in the surface waters. Compiled from Byrne and Sholkovitz (1996) and Amakawa *et al.* (2000).

leaching experiments of particulate matter and acidification treatment of both filtered and unfiltered seawaters to pH ∼ 1.5 to determine acid-soluble particulate fraction of REEs, the value of γ is deduced to be between 0.6 and 1.0. The mean residence times of REEs estimated using these values are given in **Table 3**. They range from 50 years for Ce to 2900 years for Lu. The short mean residence time of Ce is approximately equal to that of Th, being consistent with their predicted dominance of hydrolysis species in seawater. The 400 year residence time is well suited for Nd with its heterogeneous distribution of the isotopic ratios in the oceans.

It is also clear that eolian and riverine sources alone are insufficient to yield such short residence times and there must be additional sources of REEs in the ocean. The most likely candidate of the potential REE source is remineralization of nearshore, coastal and shelf sediments as described earlier. The magnitude of this remineralization flux required to balance each REE in the ocean is given in **Table 3**. Those fluxes are quite large particularly for the light REEs, whereas the relative importance of remineralization decreases and becomes somewhat comparable with the sum of eolian and riverine inputs for the heavy REEs. This REE fractionation during remineralization on the shelf may contribute the

different NPDW-normalized REE patterns observed in the surface waters (**Figure 9**), although the mechanism is not well understood.

Summary and Conclusion

Although the oceanic distributions of rare earth elements somewhat resemble those of nutrients, their behaviors are clearly different in that they are not actively taken up by photoplankton but passively scavenged by particles. Elemental reactivity with suspended particles, which controls, together with sinking of particle aggregates, the mean oceanic residence times of not only REEs but also a number of other heavy metals, is best understood by the competitive complexation reactions of dissolved REEs with ligands on the surface of particles and in solution. This yields the progressive enrichment from the light to the heavy REEs in the shale-normalized pattern as commonly observed in seawater. Remineralization of REEs from coastal and shelf sediments is thought to play a significant role in the global budget of REEs and the geochemical and isotopic consistency of Nd in the ocean. The REEs and Nd isotopes provide novel and unique oceanographic tracers or chemical problems in studying (1) particle scavenging processes, (2) redox sensitive geochemical processes with Ce, and (3) identification

and modification of water masses. Applications to the wider problems are being explored.

See also

Estuarine Circulation. River Inputs. Tracers of Ocean Productivity. Water Types and Water Masses.

Further Reading

Alibo DS and Nozaki Y (1999) Rare earth elements in seawater: particle association, shale-normalization, and Ce oxidation. *Geochimica et Cosmochimica Acta* 63: 363–372.

Alibo DS and Nozaki Y and Jeandel C (1999) Indium and yttrium in North Atlantic and Mediterranean waters: comparison to the Pacific data. *Geochimica et Cosmochimica Acta* 63: 1991–1999.

Bertram C and Elderfield H (1993) The geochemical balance of the rare earth elements and neodymium isotopes in the oceans. *Geochimica et Cosmochimica Acta* 57: 1957–1986.

Byrne RH and Sholkovitz ER (1996) Marine chemistry and geochemistry of the lanthanides. In: Gschneider Jr KA and Eyring L (eds) *Handbook on the Physics and Chemistry of Rare Earths*, vol. 23, pp. 497–593. Amsterdam: Elsevier Science.

DeBaar HJW, Bacon MP and Brewer PG (1983) Rare-earth distributions with a positive Ce anomaly in the western North Atlantic Ocean. *Nature* 301: 324–327.

Elderfield H and Greaves MJ (1982) The rare earth elements in seawater. *Nature* 296: 214–219.

German CR, Holliday BP and Elderfield H (1991) Redox cycling of rare earth elements in suboxic zone of the Black Sea. *Geochimica et Cosmochimica Acta* 55: 3553–3558.

Goldberg ED, Koide M, Schmitt RA and Smith RH (1963) Rare-earth distributions in the marine environment. *Journal of Geophysical Research* 68: 4209–4217.

Greaves MJ, Statham PJ and Elderfield H (1994) Rare earth element mobilization from marine atmospheric dust into seawater. *Marine Chemistry* 46: 255–260.

Lipin BR and McKay GH (eds) (1989) Geochemistry and mineralogy of rare earth elements. *Reviews in Mineralogy* 21, Washington, DC: Mineralogical Society of America.

Nozaki Y (1997) A fresh look at elemental distribution in the North Pacific Ocean. *EOS Transactions* 78: 221.

Nozaki Y, Alibo DS, Amakawa H, Gamo T and Hasumoto H (1999) Dissolved rare earth elements and hydrography in the Sulu Sea. *Geochimica et Cosmochimica Acta* 63: 2171–2181.

Sholkovitz ER, Landing WM and Lewis BL (1994) Ocean particle chemistry: The fractionation of rare earth elements between suspended particles and seawater. *Geochimica et Cosmochimica Acta* 58: 1567–1579.

Sholkovitz ER and Schneider DL (1992) Cerium redox cycles and rare earth elements in the Sargasso Sea. *Geochimica et Cosmochimica Acta* 55: 2737–2743.

Taylor SR and McLennan SM (1985) *The Continental Crust: Its Composition and Evolution*. Oxford: Blackwell.

RED SEA CIRCULATION

D. Quadfasel, Niels Bohr Institute, Copenhagen, Denmark

Introduction

The Red Sea is a fiord type marginal sea in the north-west of the Indian Ocean, exposed to the arid climate of northern Africa and Arabia. Strong evaporation leads to a buoyancy-driven overturning circulation and to the production of a dense and highly saline water mass, the Red Sea Water. Near the surface the circulation is substantially modified through the forcing by the monsoon winds. Red Sea water spills at a rate of $0.37 \times 10^6 \, \mathrm{m^3 \, s^{-1}}$ through the Strait of Bab El Mandeb into the Gulf of Aden and spreads at intermediate depths in the Indian Ocean, where it can be traced as far south as the southern tip of Africa. The circulation of the Red

Sea appears not to be controlled by the hydraulics in the strait. This article summarizes the circulation internal to the Red Sea, the formation and transformation of the deep water masses and the exchange of water between the Red Sea and the Gulf of Aden.

The Red Sea was created as part of the spreading rift system between the African and the Arabian plates. It stretches between $12°$ and $20°$N from tropical to subtropical latitudes (**Figure 1**), is about 2000 km long, on average 220 km wide and reaches depths of up to 2900 m, but its mean depth is only 560 m. The only connection to the oceans is in the south to the Gulf of Aden–Indian Ocean via the narrow Strait of Bab El Mandeb. The shallow Hanish sill of 163 m depth in the north of the strait limits the free communication to the upper part of the water column. Northern appendices to the Red Sea are the Gulf of Suez, a shallow shelf basin, and the 1800 m deep Gulf of Aqaba, a smaller version of the Red Sea itself, bounded by a 260 m deep sill